

Twisted ZB–CdTe/RS–PbTe (111) heterojunction as a metastable interface structure

This article has been downloaded from IOPscience. Please scroll down to see the full text article.

2012 New J. Phys. 14 113021

(<http://iopscience.iop.org/1367-2630/14/11/113021>)

View [the table of contents for this issue](#), or go to the [journal homepage](#) for more

Download details:

IP Address: 152.15.9.254

The article was downloaded on 16/02/2013 at 17:15

Please note that [terms and conditions apply](#).

Twisted ZB–CdTe/RS–PbTe (111) heterojunction as a metastable interface structure

Shuqiang Jin^{1,5}, Chunfeng Cai¹, Bingpo Zhang¹, Huizhen Wu^{1,5}, Gang Bi², Jianxiao Si³ and Yong Zhang⁴

¹ Department of Physics and State Key Laboratory for Silicon Materials, Zhejiang University, People's Republic of China

² School of Information and Electrical Engineering, Zhejiang University City College, People's Republic of China

³ Department of Physics, Zhejiang Normal University, People's Republic of China

⁴ Department of Electrical and Computer Engineering, University of North Carolina at Charlotte, Charlotte, NC 28223, USA

E-mail: jinshuqiang@zju.edu.cn and hzwu@zju.edu.cn

New Journal of Physics **14** (2012) 113021 (13pp)

Received 5 September 2012

Published 15 November 2012

Online at <http://www.njp.org/>

doi:10.1088/1367-2630/14/11/113021

Abstract. The heterostructures of (zinc-blende)–CdTe/(rock-salt)–PbTe are typically found to have their common cubic axes aligned to each other, as in the case of PbTe quantum dots embedded in a CdTe matrix. In this work, we perform both theoretical and experimental studies on the CdTe/PbTe heterostructure in a different geometry: a planar CdTe/PbTe (111) heterostructure. We simulate the epitaxial growth of CdTe (PbTe) on the (111) PbTe (CdTe) substrate, using a density-functional theory. A twisted CdTe/PbTe (111) interface structure has been predicted in the layer-by-layer epitaxial growth on the (111) substrate, in contrast to the non-twisted CdTe/PbTe (111) interface reported in the literature. This predicted structure has been confirmed experimentally in the heterostructure grown by molecular beam epitaxy, using a high-resolution transmission electron microscope. The twisted interface has a lower binding energy than the non-twisted one, indicating that the twisted structure is a metastable phase formed in

⁵ Authors to whom any correspondence should be addressed.



Content from this work may be used under the terms of the [Creative Commons Attribution-NonCommercial-ShareAlike 3.0 licence](https://creativecommons.org/licenses/by-nc-sa/3.0/). Any further distribution of this work must maintain attribution to the author(s) and the title of the work, journal citation and DOI.

the non-equilibrium growth process. Additionally, the interface reconstructions of the CdTe/PbTe (111) heterostructure observed by reflection high-energy electron diffraction are explained using the twisted interface model.

Contents

1. Introduction	2
2. Theoretical method	3
3. Experimental setup	5
4. Results and discussion	6
4.1. The growth simulation of CdTe/PbTe(111) heterojunctions	6
4.2. Interface reconstructions during growth processes	8
5. Conclusion	12
Acknowledgments	12
References	12

1. Introduction

Narrow gap PbTe is known to have superior thermoelectric and optical properties and great potential for applications in energy and light sources [1–4]. As one of the few structure-mismatched heterostructures (as opposed to the more familiar ‘lattice-mismatched’ heterostructures due to the lattice parameter difference), CdTe/PbTe heterojunctions (HJs), which were first realized through epitaxial growth by Koike *et al* [5] have attracted much attention [6, 7] since the synthesis of PbTe quantum dots (QDs) in a CdTe matrix that exhibits intensively enhanced room-temperature mid-infrared luminescence [6–10]. PbTe is in a rock-salt (RS) and CdTe in a zinc-blende (ZB) structure, but they have nearly the same crystal lattice constants: 6.46 and 6.48 Å at 300 K, respectively. Mid-infrared light-emitting diodes with epitaxial PbTe QDs in CdTe have been fabricated [3]. A large Rashba splitting is predicted in CdTe/PbTe/PbSrTe quantum wells (QWs) [11, 12], a promising structure for spintronic devices. Recently, an abnormal enhancement of mid-infrared light emission due to coupling with surface plasmons was demonstrated in a polar and structure-mismatched CdTe/PbTe (111) single heterojunction (SHJ) [4]. PbTe QDs are obtained by annealing the [100] oriented CdTe/PbTe/CdTe QWs [8]. The crystalline planes of the (100) facets of the PbTe QDs are found to be parallel to the corresponding (100) planes of CdTe, due to the constrain of the epitaxial growth of the QWs on the (100) substrate, as observed by transmission electron microscopy (TEM) [13]. The structural properties of PbTe/CdTe (100), (110) and (111) interfaces have been theoretically studied by Leitsmann *et al* [14], where an average interface energy of about 0.2 J m^{-2} (12.5 meV Å^{-2}) was found; no interface reconstruction was reported for these interfaces.

Previous CdTe/PbTe heterostructures are mostly in the form of the QDs of one component embedded in the other; the structure was typically grown on the (100) substrates. In this work, we are interested in the growth of a planar heterostructure on the (111) substrates. The equilibrium structure is more stable than other non-equilibrium structures since it has a lower total energy. However, in a non-equilibrium epitaxial growth, we usually do not get the equilibrium structure, but a metastable structure. A well-known example is the formation of partially ordered

III–V alloys during epitaxial growth [15]. There are no reports relating to the growth simulation of CdTe/PbTe (111) HJ. Because the crystal structure of the (111) plane is rather different from that of the (100) and (110) planes for both PbTe and CdTe, the interface crystal structure of the (111) heterostructure could be different from that of the (100) epitaxial structure.

It is known that not all IV–VI materials have stable RS structures and that some of them are distorted by the strong pseudo-Jahn–Teller (PJT) coupling [16, 17]. Recently, the distorted PbTe RS local structure, which behaves like that in ferroelectrically distorted lone-pair-active Pb^{2+} compounds, such as PbTiO_3 [18], was found by an atomic pair distribution function analysis at room temperature [19]. This finding implies that the RS structure PbTe may easily become unstable under certain circumstances. Nevertheless, a bulk CdTe crystal is typically an insulator with a wide band gap (1.6 eV) in the ZB structure formed by the sp^3 hybridization [20, 21]. The ZB structure has alternating interplanar spacings along the [111] direction, whereas the RS structure has equally spaced (111) planes. Modeling the structure-mismatched CdTe/PbTe (111) interfaces is not a straightforward task, because the (111) surfaces of PbTe and CdTe are polar and the atomic relaxation calculation is hard to converge due to the presence of intrinsic as well as artificial electric fields induced by the polar surfaces or interfaces. As experimentally demonstrated by Cai *et al* [4], the interfacial effect plays an important role in the strong luminescence enhancement. Therefore, it is of fundamental interest as well as pivotal for understanding the experimental observations to model the crystal structure and corresponding electronic structure of the interface for the SHJ of CdTe/PbTe.

We firstly simulate the epitaxial growth of CdTe (PbTe) on a PbTe (CdTe) (111) substrate using a density-functional theory (DFT) approach. A ‘double external field correction’ method is adopted to remove the artifacts due to the use of the supercell approach. A metastable interface structure is predicted to form in the layer-by-layer epitaxial growth. Specifically, the (111) epilayer is rotated with respect to the substrate about the [111] axis by 180° , termed a ‘twisted’ structure that has a slightly higher total energy than the ‘normal’ (non-twisted) structure. The formation of the twisted interface structure is confirmed in the materials grown by molecular beam epitaxy (MBE) using a high-resolution transmission electron microscope (HR-TEM). Interface reconstruction during the growth of the CdTe/PbTe SHJ was characterized by reflection high-energy electron diffraction (RHEED). The predicted twisted structure is expected to yield a very different electronic structure near the interface; this work lays the foundation for the future exploration of this type of unusual semiconductor heterostructure.

2. Theoretical method

A DFT approach within a generalized gradient approximation [22], implemented in a Vienna *ab initio* simulation package [23, 24], is applied to study the PbTe/CdTe interface. Spin–orbit coupling is taken into account since this effect plays an important role in materials with heavy elements, such as Pb and Te [25]. The interaction of the valence electrons with the remaining ions was modeled by pseudopotentials generated within the projector augmented wave method [26]. The Cd 4d and Pb 5d electrons are treated as valence electrons since the outermost occupied d states give rise to shallow semicore bands, which contribute to chemical bonding in IV–VI materials [27]. The heterostructure is modeled by a slab with a vacuum space of approximately 4 nm. The Brillouin zone integration is performed by a summation over Monkhorst–Pack special k -points [28]. $5 \times 5 \times 1$ k -point meshes are used for the vacuum slab modeling.

In the real material growth, for instance, the CdTe epitaxial layer is grown on a PbTe buffer layer that is first grown on a BaF₂(111) substrate. However, in the modeling, we consider only a single heterostructure such as CdTe on PbTe, without having to include the BaF₂ substrate, because in the real growth the buffer layer is rather thick (of the order of 1 μm) so the buffer layer can be viewed as the substrate.

To simulate the layer-by-layer growth process, e.g. CdTe growing on a Te terminated PbTe (111) surface, we use a 24 bi-layer PbTe as the substrate. We start the calculation with only one Cd atomic layer of CdTe on the PbTe surface, allowing the atoms to relax; we then repeat the calculation by adding a Te layer and relaxing the structure, and so on until all the desired CdTe layers are included.

Since the [111] orientations in both RS–PbTe and ZB–CdTe are polar, the combination of the two slabs leads to a supercell with chemically, structurally and electrostatically different interfaces. In the following, the surfaces (interfaces) with the directions of [111] and $\overline{[111]}$ of CdTe are labeled as *A* (Cd-terminated) and *B* (Te-terminated), respectively. To correct the artificial electric field caused by the use of the supercell approach, we propose a double external field (DEF) correction method. Taking the growth of CdTe on a PbTe (111) buffer layer as an example, when the slab contains a small number of atomic layers of PbTe and CdTe, there are three electrostatic potential (ESP) differences: $\Delta\Phi^{\text{CdTe}}$, which is induced by the CdTe surface and the CdTe/PbTe interface; $\Delta\Phi_{1,2}^{\text{vacuum}}$ induced by the PbTe surface and CdTe surface; and $\Delta\Phi^{\text{PbTe}}$ induced by the PbTe surface and the CdTe/PbTe interface. These ESP differences could be obtained by the calculation of the plane-averaged ESP along the growth orientation, as shown in figure 1(a). As a result, three different electric fields are induced along the [111] direction in the CdTe film, the vacuum layer and the PbTe layer, respectively. It is known that the ESP differences do not depend on the slab size [14, 29], which we have verified by changing the thickness of the PbTe layer in the slab model. Therefore, the electric field in the PbTe layer tends to zero when the thickness of the PbTe layer reaches infinity. As the PbTe layer would be much thicker than the CdTe film, the electric field with real physical meaning is only that in the CdTe film, as shown in figure 1(b).

To compensate the artificial electric fields in the vacuum layer and the PbTe layer, a DEF correction scheme is suggested: one external field is used to compensate the artificial electric field in the vacuum layer, which is similar to the dipole correction introduced by Neugebauer and Scheffler [30], with the additional external ESP given as

$$\Phi_V^{\text{ext}} = \frac{-(\Delta\Phi_1^{\text{vacuum}} + \Delta\Phi_2^{\text{vacuum}})}{z_{\text{max}}^V - z_{\text{min}}^V} [z - z_{\text{max}}^V \theta(z_0 - z)], \quad (1)$$

where $[z_{\text{min}}^V, z_{\text{max}}^V]$ is the interval of the vacuum region along the [111] direction and z_0 is the position with the lowest plane-averaged charge density in the vacuum region that has been set to zero in figure 1. The other external field is used to compensate the artificial electric field in the PbTe region to mimic the limit of an infinitely thick PbTe substrate. The corresponding external ESP can be written as

$$\Phi_{\text{PbTe}}^{\text{ext}} = \frac{\Delta\Phi^{\text{PbTe}}}{z_i - z_s^{\text{sub}}} \{z [\theta(z - z_s^{\text{sub}}) - \theta(z - z_i)] - z_s^{\text{sub}}\}, \quad (2)$$

here z_i and z_s^{sub} are the interface position and the bottom surface position of the PbTe along the [111] direction, respectively. In the correction procedure, the ESP differences ($\Delta\Phi_{1,2}^{\text{vacuum}}$, $\Delta\Phi^{\text{PbTe}}$) vanish self-consistently, i.e., after the self-consistent field calculation is completed the

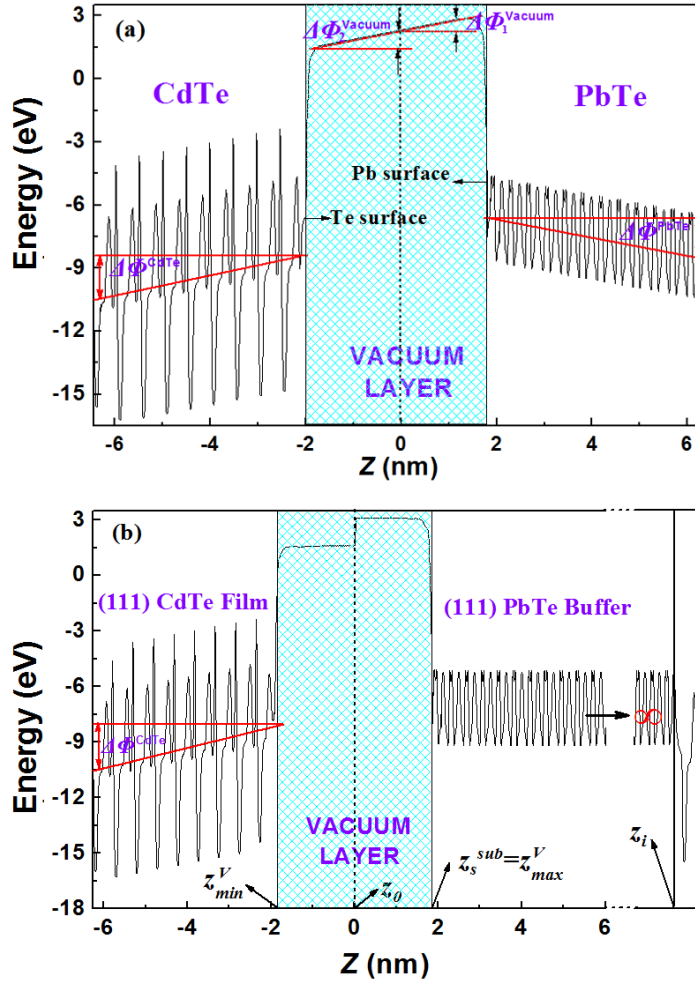


Figure 1. The plane-averaged ESP of (a) the CdTe/PbTe (111) SHJ without any correction; (b) the CdTe thin film grown on a thick PbTe layer after the double dipole correction.

initial ESP (without correction) is obtained, then the values of $\Delta\Phi^{\text{CdTe}}$, $\Delta\Phi^{\text{vacuum}}$ and $\Delta\Phi^{\text{PbTe}}$ are attained by calculating the plane-averaged ESP. The new ESP is obtained by adding the external ESP in equations (1) and (2); the total free energy is corrected by equation (3) [31]:

$$\Delta E_{\text{tot}} = \frac{1}{2} \left[\int (\Phi_{\text{PbTe}}^{\text{ext}}(\mathbf{r}) + \Phi_{\text{V}}^{\text{ext}}(\mathbf{r})) \cdot n(\mathbf{r}) d^3r - \sum_I Z_I (\Phi_{\text{PbTe}}^{\text{ext}}(\mathbf{R}_I) + \Phi_{\text{V}}^{\text{ext}}(\mathbf{R}_I)) \right], \quad (3)$$

where Z_I is the valence and \mathbf{R}_I is the position of the I th ion, which leads to a new electron density $n(\mathbf{r})$. The ESP should be calculated again using the new electron distribution. This procedure continues until the ESP differences $\Delta\Phi_{1,2}^{\text{vacuum}}$ and $\Delta\Phi^{\text{PbTe}}$ are smaller than a tolerant value.

3. Experimental setup

We grew the PbTe(CdTe)/CdTe(PbTe) HJ sample by solid-source MBE using a different growth process (i.e., CdTe on PbTe or PbTe on CdTe). The PbTe/CdTe HJs were grown on CdTe (111)

single-crystal substrates, which were cut along the [111] direction into $800\ \mu\text{m}$ thick slices. Because of the big difference between the thermal expansion coefficients of CdTe and PbTe ($\alpha_{\text{CdTe}} = 4.9 \times 10^{-6}\ \text{K}^{-1}$, $\alpha_{\text{PbTe}} = 19.8 \times 10^{-6}\ \text{K}^{-1}$), the $1\ \mu\text{m}$ thick PbTe film was grown at 648 K and slowly cooled down to room temperature, which can effectively reduce the interface defects caused by the thermal stress relaxation. To observe the interface structure of PbTe/CdTe HJ we performed HR-TEM characterization on a cross-sectional specimen along the $\langle 110 \rangle$ zone axis. For the CdTe/PbTe HJ, a $1\ \mu\text{m}$ PbTe buffer layer was first grown on BaF_2 (111) substrates at 620 K and then a CdTe layer was grown on the PbTe buffer at 520 K. The interface reconstruction during the growth process was observed by the RHEED patterns.

4. Results and discussion

4.1. The growth simulation of CdTe/PbTe(111) heterojunctions

To determine the favorable interface structures for different growth processes (i.e., CdTe on PbTe or PbTe on CdTe), we perform the relaxation calculation using the DEF correction method. The [111]-oriented layer (either PbTe or CdTe) is simulated by passivating the dangling bonds of its bottom surface using pseudo-hydrogen atoms to remove the influence of the bottom surface states. Twenty-four bi-layers are used for the buffer material in the slab. The atomic geometries are obtained by atomic position relaxation until the Hellmann–Feynman forces are smaller than $10\ \text{meV}\ \text{\AA}^{-1}$.

In contrast to interfaces *A* and *B* of the PbTe QDs embedded in the CdTe matrix [8], in which the PbTe crystal planes are parallel to corresponding planes of CdTe (e.g. (100) plane) as shown in figures 2(a) and (c), we have found a twisted interface structure in the layer-by-layer non-equilibrium growth, as illustrated in figures 2(b) and (d). For clarity in the comparison of the PbTe QDs embedded in the CdTe matrix and the PbTe/CdTe HJs, the atomic displacements are not included in figure 2. Specifically, the new structure is constructed by rotating the PbTe lattice in figures 2(a) and (c) around the [111] axis by 180° ; therefore, the CdTe (100) and PbTe (100) planes are inclined with respect to each other by an angle that is twice that between [111] crystal orientation and (100) plane ($\arccos(\sqrt{2/3})$). Thereafter, we refer to the PbTe/CdTe interface structures in figures 2(b) and (d) as twisted interfaces *A* and *B*, respectively. For convenience, the PbTe and CdTe (111) atomic layers are labeled as *A(B)-P1*, *A(B)-P2*, ..., and *A(B)-C1*, *A(B)-C2*, ... originating from the interface *A(B)*, respectively.

When CdTe grows on the PbTe (111) layer, which is simulated by sequentially adding Cd and Te layers on the PbTe slab, the calculation shows that it forms the twisted interface *A* structure, no matter which layer (Pb or Te) terminates the PbTe (111) surface. It is understandable that the Pb terminated PbTe surface is first followed by a Te layer, because Pb and Cd atoms do not bond directly. The Te atoms form ionic bonds with the Pb atoms on the surface, which continues the RS structure. Since the interplanar spacings of PbTe are equal, the tellurided Pb terminated PbTe (111) surface is equivalent to a Te terminated PbTe surface. However, when PbTe grows on a CdTe (111) layer, there are two possibilities (i.e. surfaces *A* and *B*) because the (111) interplanar spacings of the Cd layers and Te layers are not equal to each other, which results in formation of two different PbTe/CdTe interface structures when the PbTe layer grows on the *A* and *B* surfaces of the CdTe. Our simulation shows that it forms the structure of a twisted interface *A* (*B*) when the PbTe grows on the CdTe surface *A* (*B*).

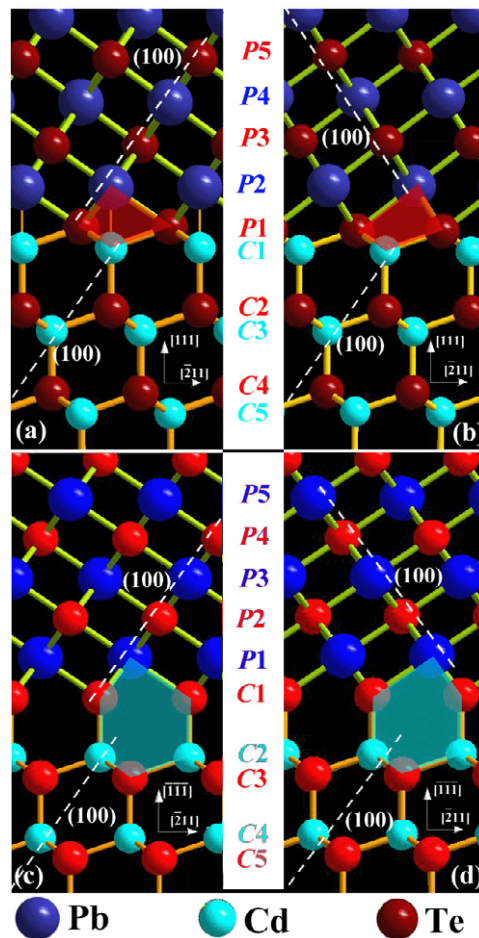


Figure 2. The PbTe/CdTe (111) interface A and B structures of the PbTe QDs embedded in CdTe ((a), (c)), [13] and the PbTe/CdTe (111) HJs ((b), (d)).

Compared to the structure in figures 2(a) and (c), the twisted structures keep the RS structure, PbTe, and the ZB structure, CdTe, as close as possible to their bonding situations in the bulks near the interface. For example, the PbTe (CdTe) structure consists of periodic rectangles (hexagons), but the shapes of the rectangles (hexagons) at the interface (one side of which is formed by the Cd–Te (Pb–Te) bonds) are quite different (see figures 2(a) and (c)). The twisted structure in figures 2(b) and (d) mostly keeps the bulk shape of the rectangles (hexagons), whereas the non-twisted structure in figures 2(a) and (c) evidently changes the bulk shape of the rectangles (hexagons) as highlighted in figure 2. At this point, the twisted structure forms more easily in the epitaxial growth than the non-twisted one at the interface.

Next we compare the total energies or the binding energies of the two types of interface structures. The equation below is used to calculate the binding energy

$$E_{\text{binding}} = E_{\text{tot}}(\text{PbTe}) + E_{\text{tot}}(\text{CdTe}) - E_{\text{tot}}(\text{CdTe/PbTe}), \quad (4)$$

where the three terms are respectively the total energy of the PbTe, CdTe, and CdTe/PbTe slab. PbTe or CdTe slabs each consist of 24 (111) bi-layers. The twisted and non-twisted heterostructures are calculated in the dipole corrected stoichiometric slab approximation [29]. To keep the system stoichiometric, it is necessary to have both interface A and B in the same slab.

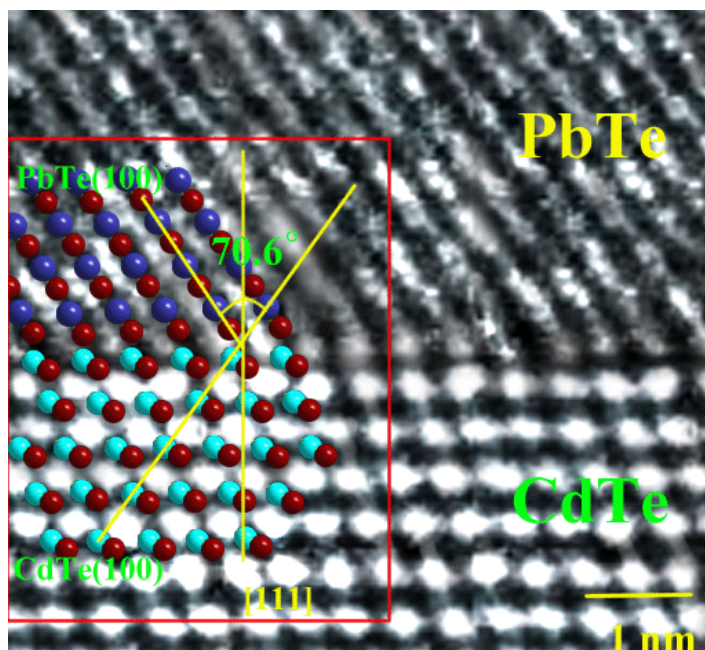


Figure 3. The HR-TEM image of a twisted interface *B*. The atomic arrangements in the PbTe/CdTe HJ are illustrated in the inset panel overlaid on the TEM picture.

It turns out that the binding energy for the non-twisted interface ($24.0 \text{ meV } \text{\AA}^{-2}$) is larger than that of the twisted one ($21 \text{ meV } \text{\AA}^{-2}$), which indicates that the non-twisted interface structure is the energetically favorable equilibrium phase and the twisted one is a metastable phase formed in the non-equilibrium growth process. As a matter of fact, a metastable phase is often observed in the non-equilibrium epitaxial growth by MBE and MOCVD; for instance, a well-known phenomenon, spontaneous ordering, has been observed in the epitaxial growth of a semiconductor alloy, GaInP on GaAs in particular [32].

The twisted interface structure is observed by our HR-TEM measurement in a PbTe/CdTe SHJ grown by MBE, as shown in figure 3. The inset of figure 3 illustrates the atomic arrangements near the interface. The inclined angle between the (100) planes of PbTe and CdTe is 70.6° ($2 \arccos(\sqrt{2/3})$). We note that because of the twisted interface structure, it is not feasible to form rhombocubo-octahedral PbTe QDs by annealing the [111] oriented CdTe/PbTe/CdTe QWs.

4.2. Interface reconstructions during growth processes

The PJT coupling in PbTe can be sensitively dependent on the tensile strain [33]. According to our relaxation calculation for the bulk PbTe and CdTe, the lattice constant of these two materials is 6.422 and 6.647 \AA (0 K), respectively, and the lattice mismatch ε of the PbTe(CdTe)/CdTe(PbTe) HJs is 0.7% . Therefore, PbTe has a small tensile strain and the RS structure of the PbTe may be distorted by PJT coupling at the interface. The vacuum slab with 2×2 lateral unit cells is used to test the interface reconstruction while the relaxation is only allowed along the growth direction. Simulation shows that bulk PbTe has equal interplanar

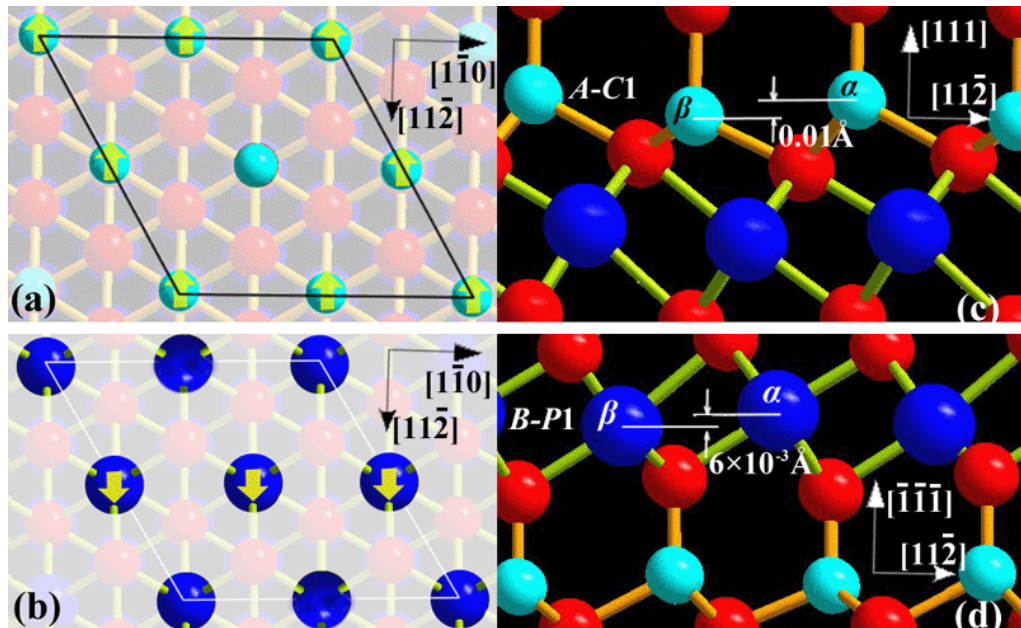


Figure 4. (a), (c) The reconstruction of the first Cd layer on the PbTe buffer; (b), (d) the reconstruction of the first Pb layer on the CdTe (111) interface *B*.

spacings (1.85 \AA at 0 K) along the $[111]$ direction. However, at the interface of PbTe/CdTe HJ, the PJT coupling drives the Pb and Te fcc sub-lattices of the RS structure deviated slightly from each other along the $[111]$ direction by 0.3 \AA due to the tensile strain. As a result, the interplanar spacings of PbTe (111) at the interface region become alternately wide (2.15 \AA) and narrow (1.55 \AA), which is called rhombohedral distortion [33].

The non-twisted (111) interface of the PbTe QDs in the CdTe matrix gives no evidence for an interface reconstruction [14]. However, the twisted structure in the CdTe/PbTe (111) HJ induces reconstruction due to the competition between the RS structure and ZB structure at the interface. We notice that one of four atoms from different lateral unit cells in the same atomic layer has a vertical displacement compared to the other three atoms when CdTe is grown on the PbTe (111), as shown in figures 4(a) and (c). The vertical displacement in the first Cd layer is 0.01 \AA , it gradually diminishes within a few bi-layers, which means that a 2×2 reconstruction is formed at interface *A*. For interface *B*, we obtain a 2×1 reconstruction, as shown in figure 4(d), but the maximum vertical displacement is extremely small, $\sim 6 \times 10^{-3} \text{ \AA}$.

The interface reconstruction is a result of the competition between the RS structure and ZB structure at the interface. As illustrated in figure 4(c), when CdTe grows on the surface of PbTe (111), $3/4$ of the Cd atoms (α atoms) of the *A-C1* layer come up from the *A-C1* plane trying to form the RS lattice with the Te atoms in the *P1* layer, while leaving other Cd atoms almost keeping the ZB lattice with the Te atoms. Shown in figure 4(d), when the PbTe grows on the surface *B* of CdTe (111), one half of the Pb atoms (β atoms) of the *B-P1* layer go down slightly from the plane, trying to form the ZB lattice with the Te atoms in the *B-C1* layer. It is well known that Pb and Te atoms form ionic bonds in bulk PbTe, whereas Cd and Te atoms form mostly covalent bonds in bulk CdTe. Compared to the bulk PbTe and CdTe crystals, the bonds around the CdTe/PbTe interface cannot be described simply by either an ionic or covalent character since both the Pb–Te and Cd–Te bonds are covalent bonds with a partial

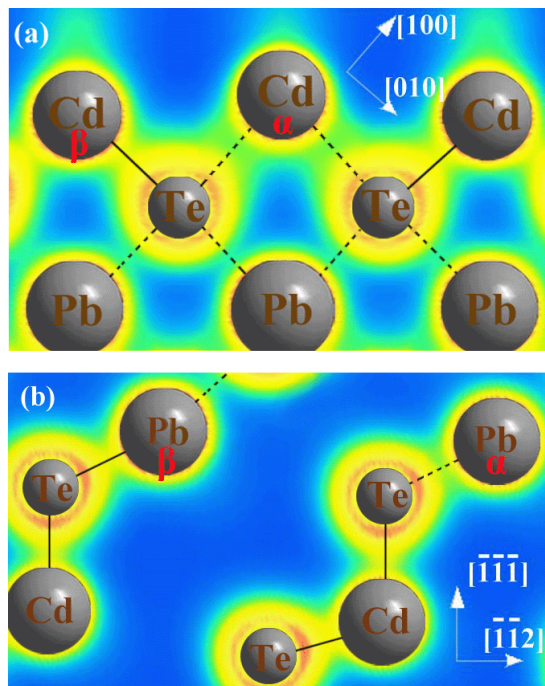


Figure 5. The electron density distributions at the twisted interfaces A (a) and B (b) with reconstructions for PbTe grown on CdTe. The ionic-like bonds and covalent-like bonds are indicated by the dashed and solid lines, respectively.

ionic property. Figure 5 shows the calculated electron density around the interface, showing that the Cd atoms, which come up from the C1 layer, form Cd–Te bonds in more of an ionic nature than the other Cd atoms at interface A (the atom α in figure 5(a)), and the lower Pb atoms form Pb–Te bonds in more of a covalent nature than the other Pb atoms at interface B (the atom β in figure 5(b)), which explains the competition between RS and ZB structures at the interface. In order to enhance the color contrast, the Cd 4d and Pb 5d electron densities, which are highly localized around the Cd and Pb ion cores, are not displayed (under the gray atom balls).

Our simulation predicts that the surface of a CdTe (111) B layer has a weak 2×1 surface reconstruction. The reconstruction is caused by the distortion of the sp^3 dangling bonds on the CdTe (111) surface, which is analogous to the 2×1 surface reconstruction on a Si (111) surface. Figure 6(a) shows the RHEED pattern measured from the CdTe (111) surface B along the $[1\bar{1}0]$ direction. The narrow faint fringes are the reconstruction lines, which disappear in the measured RHEED pattern along the $[11\bar{2}]$ direction. The reconstruction fringes fade away as soon as PbTe grows on it, as shown in figure 6(b), because the vertical displacement in the PbTe layers is too small to be discriminated at the interface B. The surface of a PbTe (111) does not show any reconstructions, as illustrated in figure 6(c). However, bright reconstruction fringes appear as soon as CdTe grows on it, as observed by RHEED patterns shown in figure 6(d) along both the $[1\bar{1}0]$ and $[11\bar{2}]$ directions, which implies a 2×2 reconstruction at the twisted interface A. It is also noted that the reconstruction fringes are very bright at the growth temperature (~ 520 K), but they gradually become weaker and weaker as the temperature decreases. According to our calculation, for the PbTe grown on the CdTe (111) B surface at 0 K, the RS structure of PbTe

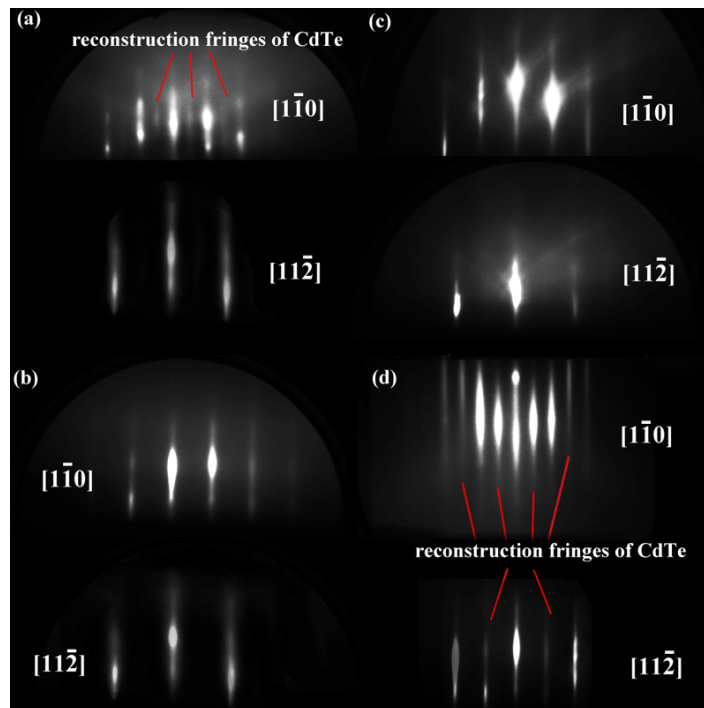


Figure 6. The RHEED patterns of CdTe and PbTe: (a) the surface *B* of a CdTe (111) substrate; (b) the surface at the instant the beginning of the PbTe grew on the surface *B* of CdTe (111); (c) the surface of a PbTe (111) buffer; (d) the surface at the instant the beginning of the CdTe grew on the PbTe (111) surface. The directions labeled in addition to the patterns are the glancing incident directions of the electron beam.

is distorted by both the tensile strain and the rhombohedral distortion due to the PJT coupling in PbTe. However, for the CdTe grown on the PbTe (111) surface at 0 K, the ZB structure of CdTe is only slightly distorted by the compressive strain. As a result, the vertical atom displacement at the PbTe/CdTe HJ is smaller ($\sim 6 \times 10^{-3} \text{ \AA}$) than that at the CdTe/PbTe HJ (0.01 \AA) at 0 K, as shown in figure 4, which implies a stronger distortion of the RS or ZB structure will restrain the competition between the two lattice structures at the interface. When the CdTe grows on the PbTe (111) surface, at the growth temperature ($\sim 520 \text{ K}$), the CdTe and PbTe are perfectly lattice matched ($\varepsilon < 0.05\%$). Thus the distortion caused by the strain vanishes and the vertical displacements become much larger since the competition between RS and ZB structures becomes stronger. Instead of partial ionic bonds, the α atoms of the *A-C1* layer in figure 4(c) may form an RS structure with fully ionic bonds. Furthermore, when the PbTe grows on the CdTe (111) *B* surface at 620 K, the lattice mismatch becomes greater ($\varepsilon > 0.16\%$) and the competition between the two lattice structures is restrained again, which explains why we cannot see the reconstruction fringes of the RHEED pattern in figure 6(b). Based on both the theoretical calculation for 0 K and the RHEED patterns at a high temperature, we can conclude that the vertical atom displacement is quite small ($\sim 0.01 \text{ \AA}$) at 0 K, but it becomes larger with the increasing temperature and reaches a maximum value around 500 K.

5. Conclusion

The structural properties of twisted CdTe/PbTe (111) polar interfaces are investigated both theoretically and experimentally. The epitaxial growth of CdTe (PbTe) on a polar PbTe (CdTe) surface is simulated by DFT calculations and a preferred twisted CdTe/PbTe (111) interface structure is predicted and verified by HR-TEM observation in the MBE grown PbTe/CdTe SHJ. Interface reconstructions of CdTe/PbTe (111) induced by the twisted structure are observed by RHEED and interpreted by theoretical modeling. The twisted interface structure is a metastable phase, as compared to the non-twisted structure. The formation of this metastable structure is the result of the non-equilibrium growth process, similar to the observation of spontaneous ordering in various III–V semiconductor alloys that is also driven by the surface effect. We expect that the twisted interface will yield interesting physics to be explored in comparison with the normal interface.

Acknowledgments

This work was supported by the National Key Basic Research Program of China (no. 2011CB925603) and Natural Science Foundation of China (nos 61290305, 91021020 and 61275108). The work at UNC-Charlotte was supported by a Bissell Distinguished Professorship.

References

- [1] Delaire O *et al* 2011 *Nature Mater.* **10** 614
- [2] Costi T A and Zlatic V 2012 *Phys. Rev. Lett.* **108** 036402
- [3] Hochreiner A, Schwarzl T, Eibelhuber M, Heiss W, Springholz G, Kolkovsky V, Karczewski G and Wojtowicz T 2011 *Appl. Phys. Lett.* **98** 021106
- [4] Cai C, Jin S, Wu H, Zhang B, Hu L and McCann P J 2012 *Appl. Phys. Lett.* **100** 182104
- [5] Koike K, Tanite T and Yano M 2001 *Proc. NGS 10 IPAP Conf. Series* **1** 39
- [6] Leitsmann R and Bechstedt F 2008 *Phys. Rev. B* **78** 205324
- [7] Groiss H, Hesser G, Heiss W, Schäffler F, Leitsmann R, Bechstedt F, Koike K and Yano M 2009 *Phys. Rev. B* **79** 235331
- [8] Heiss W, Groiss H, Kaufmann E, Böberl M, Springholz G, Schäffler F, Koike K, Harada H and Yano M 2006 *Appl. Phys. Lett.* **88** 192109
- [9] Leitsmann R and Bechstedt F 2009 *Phys. Rev. B* **80** 165402
- [10] Schwarzl T, Kaufmann E, Springholz G, Koike K, Hotei T, Yano M and Heiss W 2008 *Phys. Rev. B* **78** 165320
- [11] Jin S, Wu H and Xu T 2009 *Appl. Phys. Lett.* **95** 132105
- [12] Hasegawa M M and de Andrada e Silva E A 2003 *Phys. Rev. B* **68** 205309
- [13] Leitsmann R, Ramos L E, Bechstedt F, Groiss H, Schäffler F, Heiss W, Koike K, Harada H and Yano M 2006 *New J. Phys.* **8** 317
- [14] Leitsmann R, Ramos L E and Bechstedt F 2006 *Phys. Rev. B* **74** 085309
- [15] Batyrev I G, McMahon W E, Zhang S B, Olson J M and Wei S-H 2005 *Phys. Rev. Lett.* **94** 096101
- [16] Maksimenko O B and Mishehenko A S 1994 *Solid State Commun.* **92** 797
- [17] Waghmare U V, Spaldin N A, Kandpal H C and Seshadri R 2003 *Phys. Rev. B* **67** 125111
- [18] Kwei G H, Billinge S J L, Cheong S-W and Saxton J G 1995 *Ferroelectrics* **164** 57
- [19] Božin E S, Malliakas C D, Souvatzis P, Proffen T, Spaldin N A, Kanatzidis M G and Billinge S J L 2010 *Science* **330** 1660

- [20] Su C-H 2008 *J. Appl. Phys.* **103** 084903
- [21] Segall B, Lorenz M R and Halsted R E 1962 *Phys. Rev.* **129** 2471
- [22] Perdew J P, Ruzsinszky A, Csonka G I, Vydrov O A, Scuseria G E, Constantin L A, Zhou X and Burke K 2008 *Phys. Rev. Lett.* **100** 136406
- [23] Kresse G and Furthmüller J 1996 *Comput. Mater. Sci.* **6** 15
- [24] Kresse G and Furthmüller J 1996 *Phys. Rev. B* **54** 11169
- [25] Hobbs D, Kresse G and Hafner J 2000 *Phys. Rev. B* **62** 11556
- [26] Kresse G and Joubert D 1999 *Phys. Rev. B* **59** 1758
- [27] Wei S-H and Zunger A 1988 *Phys. Rev. B* **37** 8958
- [28] Monkhorst H J and Pack J D 1976 *Phys. Rev. B* **13** 5188
- [29] Leitsmann R and Bechstedt F 2007 *Phys. Rev. B* **76** 125315
- [30] Neugebauer J and Scheffler M 1992 *Phys. Rev. B* **46** 16067
- [31] Bengtsson L 1999 *Phys. Rev. B* **59** 12301
- [32] Mascarenhas A (ed) 2002 *Spontaneous Ordering in Semiconductor Alloys* (New York: Kluwer)
- [33] An J, Subedi A and Singh D J 2008 *Solid State Commun.* **148** 417